Protein-based emulsion electrosprayed micro- and submicroparticles for the encapsulation and stabilization of thermosensitive hydrophobic bioactives

Laura G. Gómez-Mascaraque, Amparo López-Rubio*

Food Quality and Preservation Department, IATA-CSIC, Avda. Agustin Escardino 7, 46980 Paterna, Valencia, Spain

*Corresponding author: Tel.: +34 963900022; fax: +34 963636301

E-mail address: amparo.lopez@iata.csic.es (A. López-Rubio)

ABSTRACT

This work shows the potential of emulsion electrospraying of proteins using food-grade emulsions for the microencapsulation and enhanced protection of a model thermosensitive hydrophobic bioactive. Specifically, gelatin, a whey protein concentrate (WPC) and a soy protein isolate (SPI) were compared as emulsion stabilizers and wall matrices for encapsulation of α-linolenic acid. In a preliminary stage, soy bean oil was used as the hydrophobic component for the implementation of the emulsion electrospraying process, investigating the effect of protein type and emulsion protocol used (i.e. with or without ultrasound treatment) on colloidal stability. This oil was then substituted by the ω-3 fatty acid and the emulsions were processed by electrospraying and spray-drying, comparing both techniques. While the latter resulted in massive bioactive degradation, electrospraying proved to be a suitable alternative, achieving microencapsulation efficiencies (MEE) of up to ~70%. Although gelatin yielded low MEEs due to the need of employing acetic acid for its processing by electrospraying, SPI and WPC achieved MEEs over 60% for the non-sonicated emulsions. Moreover, the degradation of α-linolenic acid at 80ºC was significantly delayed when encapsulated within both matrices. Whilst less than an 8% of its alkene groups were detected after 27 hours of thermal treatment for free α-linolenic acid, up to 43% and 67% still remained intact within the electrosprayed SPI and WPC capsules, respectively.

39 KEYWORDS

40 Emulsion electrospraying; spray-drying; emulsion; encapsulation; omega-3; fatty acid;

41 linolenic acid; functional food

[1] ABBREVIATIONS:

WPC: Whey protein concentrate
SPI: Soy protein isolate
MEE: Microencapsulation efficiency
ALA: α-linolenic acid
O/W: Oil in water
GRAS: Generally Recognized as Safe
Gel: Gelatin
SBO: Soy bean oil
DLS: Dynamic light scattering
CI: Creaming index
SEM: Scanning electron microscopy
FT-IR: Fourier transform infrared
TGA: Thermogravimetric analysis
DTG: Derivative thermogravimetric curves
HSH: High-speed homogenization
US: Ultrasound

1. Introduction

One of the most promising approaches to preserve hydrophobic bioactive ingredients in food systems is their nano- or microencapsulation within protective matrices (Dube, Ng, Nicolazzo, & Larson, 2010), as they act as barriers, thus limiting direct contact of the bioactives with the detrimental agents of the environment (Ye, Cui, Taneja, Zhu, & Singh, 2009). Moreover, microencapsulation can also help overcoming the incompatibility between the hydrophobic compounds and the aqueous matrix of many food products, potentially increasing their bioavailability (Braithwaite et al., 2014). However, it also represents an additional challenge, given that the use of aqueous media for the dissolution or suspension of the polymers to be used as encapsulating matrices is almost imperative for the production of edible products, in order to avoid toxicity issues (López-Rubio & Lagaron, 2012). A plausible strategy to disperse the lipophilic bioactive into the aqueous polymer solution is to prepare oil-in-water (O/W) emulsions prior to microencapsulation. Although O/W emulsions are, in general, thermodynamically unstable (McClements, 2012) there are several strategies which can be used to increase their stability and the subsequent encapsulation efficiency (Bock, Dargaville, & Woodruff, 2012), such as reducing the size of the oil droplets or addition of tensioactive compounds (Malaki Nik, Wright, & Corredig, 2010). Spray-drying is the most commonly used technology in the food industry to obtain dry encapsulation structures from emulsions (Gharsallaoui, Roudaut, Chambin, Voilley, & Saurel, 2007). However, spray-drying involves the use of a hot gas stream to rapidly dry the fine droplets produced in its initial atomization step, which results detrimental for hydrophobic thermosensitive bioactives such as ω-3 fatty acids. In contrast, electrospraying (i.e. a technique based on the electrohydrodynamic processing of polymer melts, solutions or dispersions) can be performed under mild conditions

67 (López-Rubio & Lagaron, 2012), so it has recently been proposed as an alternative for
68 the microencapsulation of labile bioactive agents (Bock et al., 2012) with promising
69 applications in the field of functional foods (Gómez-Mascaraque, Lagarón, & López-
70 Rubio, 2015; Pérez-Masiá, Lagaron, & Lopez-Rubio, 2015; Pérez-Masiá et al., 2015).
71 This technology allows the production of nano- and microencapsulation structures by
72 subjecting the polymeric fluid, which is pumped through a conductive capillary, to a
73 high voltage electric field. As a result, a charged polymer jet is ejected towards the
74 opposite electrode, which is broken down into fine droplets during the flight, generating
75 dry polymeric particles upon solvent evaporation before being deposited on the
76 collector (Bhardwaj & Kundu, 2010; Bhushani & Anandharamakrishnan, 2014;
77 Chakraborty, Liao, Adler, & Leong, 2009). Emulsion electrospraying has been recently
78 proposed for drug encapsulation (Wang, Zhang, Shao, & Wang, 2013) and for the
79 development of cytocompatible microcapsules (Song, Chan, Ma, Liu, & Shum, 2015)
80 using carbohydrate matrices, but to the best of our knowledge only the electrospraying
81 of whey protein concentrate (WPC)-stabilized emulsions has been reported for the
82 microencapsulation and protection of bioactive compounds of interest in functional
83 foods (Pérez-Masiá et al., 2015) to date.

84 Proteins are particularly interesting molecules for emulsion electrospraying, as their
85 amphiphilic structures allow their use as effective emulsifiers (McClements, 2004) in
86 addition to their primary function as wall materials. Indeed, proteins are often used as
87 ingredients in food emulsions, providing both electrostatic and steric stabilization, in
88 addition to their own nutritional properties (Malaki Nik et al., 2010).

89 In this work, three different protein types, specifically gelatin, a whey protein
90 concentrate (WPC) and a soy protein isolate (SPI) were used as encapsulation matrices
91 of α-linolenic acid (ALA) as a model hydrophobic bioactive by the emulsion

electrospraying technique, with the aim of comparing their protection ability against oxidation. ALA was chosen for this purpose as, apart from being one of the most relevant ω-3 fatty acids playing an important role in the regulation of cellular functionality (Crawford et al., 2000) and the preservation of the cardiovascular, neurovascular and mental health (Nguemeni, Gouix, Bourourou, Heurteaux, & Blondeau, 2013), it is highly susceptible to oxidative degradation when exposed to oxygen, light and/or heat (Umesha, Monahar, & Naidu, 2013). In fact, ALA is considered to be the most important precursor of flavor reversion (i.e. development of off-flavors) (Frankel, 1980) and, thus, its high instability can compromise not only the nutritional value of ALA-enriched food products but also their sensorial properties, reducing their shelf-life (Habib, Amr, & Hamadneh, 2012). Furthermore, the well-established spray-drying technique was used to dry the emulsions for comparison purposes. Two emulsification protocols were carried out prior to microencapsulation using both techniques, and the influence of emulsion properties, drying technique and type of protein on the microencapsulation efficiency and on the stabilization of ALA against degradation at high temperatures were studied.

2. Materials and Methods

2.1. Materials

Whey protein concentrate (WPC), under the commercial name of Lacprodan® DI-8090 and with a w/w composition of ~80% protein, ~9% lactose and ~8% lipids, was kindly donated by ARLA (ARLA Food Ingredients, Viby, Denmark). Soy protein isolate (SPI) was kindly donated by The Solae Company (Switzerland). Type A gelatin from porcine skin (Gel), with reported gel strength of 175 g Bloom, soy bean oil (SBO), α-linolenic

116 acid (≥99%) (ALA), Tween® 20 and potassium bromide FTIR grade (KBr) were
117 obtained from Sigma-Aldrich. 96% (v/v) acetic acid (Scharlab) was used as received.

118

119 **2.2. Preparation of oil in water (O/W) emulsions**

120 The aqueous phase of each emulsion consisted of a protein solution/dispersion. Three
121 different proteins were used to prepare the O/W emulsions: gelatin (Gel), soy protein
122 isolate (SPI) and whey protein concentrate (WPC). In a preliminary stage, soy bean oil
123 (SBO) was used as the oily phase in order to optimize the production of the
124 encapsulating structures containing lipophilic compounds, using an inexpensive oil.
125 Afterwards, SBO was substituted by a ω-3 fatty acid, linolenic acid (ALA), as a model
126 functional oil. In all cases, the oil was added in a proportion of 10% (w/w) with respect
127 to the total mass of non-volatile compounds in the capsules. The use of a surfactant,
128 Tween20®, was also considered for the stabilization of some of the emulsions, as
129 described below. The preparation of the O/W emulsions using each of the three different
130 proteins was slightly different, as illustrated in Figure 1.

131 The emulsification step itself was conducted using two different procedures. The first
132 one consisted of a one-step high-speed homogenization process conducted using an IKA
133 T-25 Digital ULTRA-TURRAX® equipped with a S 25N - 25F dispersing element
134 whose stator diameter was 25 mm (Germany) at 6000 rpm during 2 min. The other
135 approach included a second step consisting of an ultrasonication treatment, which was
136 aimed at reducing the drop size of the oil phase. For this purpose, an ultrasonic probe
137 (Bandelin electronic, Germany) was used at an amplitude of 10% and a frequency of 20
138 kHz for 2 min, in intervals of 30 s to avoid excessive heating. An ice bath was also used
139 to prevent overheating of the samples.

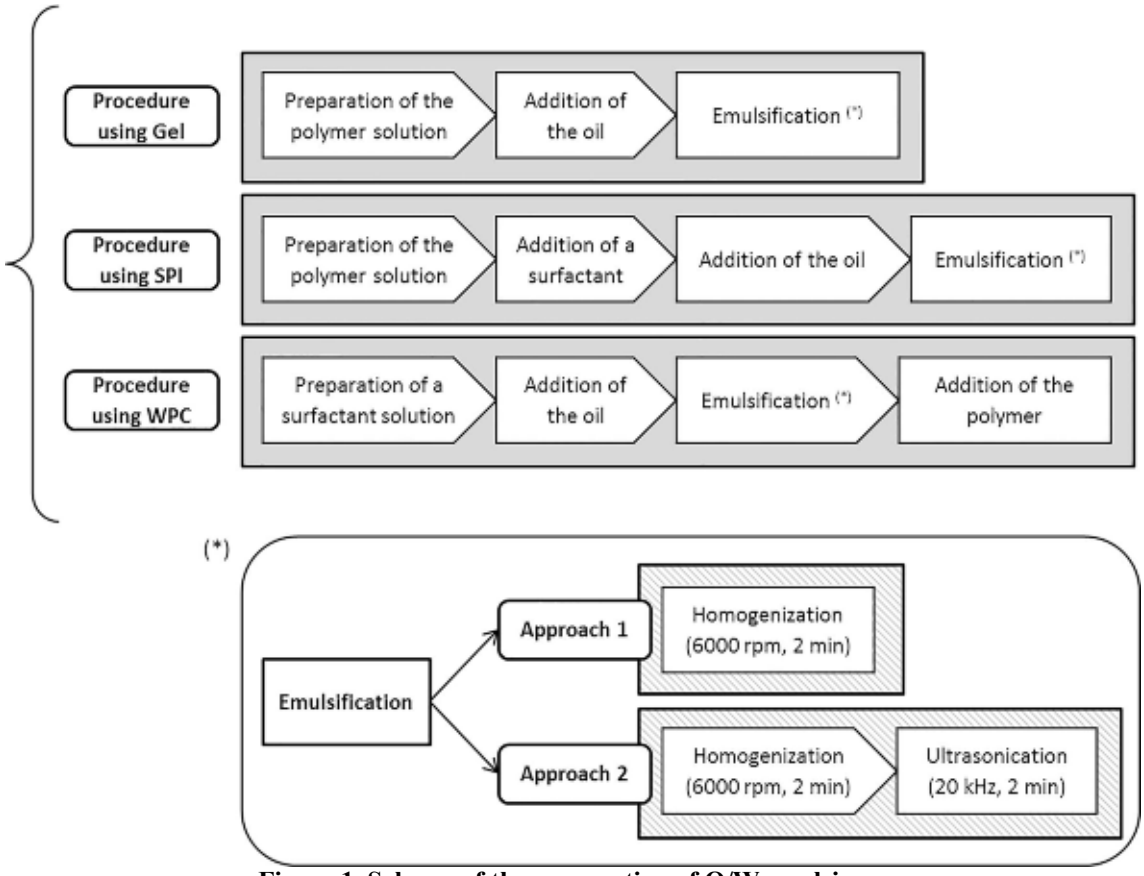

Figure 1. Scheme of the preparation of O/W emulsions

2.2.1. Preparation of O/W emulsions using gelatin

Gelatin aqueous solutions (8% w/v) were prepared as described in (Gómez-Mascaraque, Lagarón, & López-Rubio, 2015) and cooled down to room temperature before preparation of the emulsions. The use of a surfactant for the formation of stable emulsions was not necessary in this case. In fact, preliminary optimization tests showed that the addition of either Tween20® or soy lecithin as surfactants resulted in the coalescence of the oil droplets, due to the aggregation of the protein and the surfactant molecules at acidic pH. Conversely, the emulsions were stable for weeks when gelatin was used alone, both as emulsifier and as wall matrix for the capsules. Consequently, the oil phase was directly incorporated to the premix and the emulsions were prepared following both approaches described in Figure 1.

2.2.2. Preparation of O/W emulsions using SPI

SPI (10% w/v) was dissolved in distilled water and denaturation of the protein was carried out to improve its electrosprayability (Pérez-Masiá, Lagaron, & López-Rubio, 2014), by heating the solution to 90ºC for 30 min. Then, the solution was cooled down to room temperature in an ice bath before preparation of the emulsions. The addition of the surfactant Tween20® (5% w/v) was necessary to obtain stable emulsions in this case. Lastly, the oil phase was added to the premix and the emulsions were prepared following both approaches described in Figure 1.

2.2.3. Preparation of O/W emulsions using WPC

The preparation of SBO/WPC emulsions has already been reported for the encapsulation of lipophilic bioactive ingredients (Pérez-Masiá, Lagaron, & Lopez-Rubio, 2015). Based on this work, an aqueous surfactant solution was first prepared by dissolving 5 % (w/v) of Tween20® in distilled water. Afterwards, the oil phase was added, and pre-emulsions were prepared following both approaches described in Figure 1. Lastly, the required mass of WPC to achieve a protein concentration of 20% (w/v) in the aqueous phase was added to the preformed emulsions and magnetically stirred until a homogeneous emulsion was obtained.

2.3. Characterization of the emulsions

The rheological behaviour of the emulsions at 20ºC ± 0.1ºC was studied using a rheometer model AR-G2 (TA Instruments, USA) with a parallel plate geometry, using the methodology described in Gómez-Mascaraque et al. (2015) after equilibrating the samples for 2 min. All measurements were made at least in triplicate.

In addition, optical microscopy images were taken using a digital microscopy system (Nikon Eclipse 90i) fitted with a 12 V, 100 W halogen lamp and equipped with a digital camera head (Nikon DS-5Mc). Nis Elements software was used for image capturing.

2.4. Stability of the emulsions

The stability of the emulsions was assessed following the creaming index method proposed in (Surh, Decker, & McClements, 2006). Briefly, each emulsion was transferred into a sealed tube and stored for 5, 24 and 48 h at room temperature. When the emulsions separated into two different phases, the height of the top opaque ('cream') layer was measured (H_c), and the creaming index (CI) was calculated following Eq. (1):

$$CI = 100\ (H_c/H_E) \qquad \text{Eq. (1)}$$

where H_E is the total height of each emulsion in the tube.

2.5. Production of microencapsulation matrices by spray-drying

The emulsions were diluted 20-fold in distilled water prior to their processing by spray-drying, to avoid too high viscosities which would block the spraying head. The emulsions were subsequently fed to a Nano Spray Dryer B-90 apparatus (Büchi, Switzerland) equipped with a 7.0 µm pore diameter cap. The inlet air temperature was set at 90ºC, as it proved to be enough to achieve complete drying of the particles at an inlet air flow of 146 ± 4 L/min and a reduced pressure of 50 ± 3 mbar. Under these conditions, the outlet air temperature varied between 50 and 65ºC. The spray-dried

198 powders were deposited on the collector electrode by means of an applied voltage of 15
199 kV.

200

201 **2.6. Production of microencapsulation matrices by emulsion electrospraying**

202 The emulsions were processed without further dilution using a homemade
203 electrospinning/electrospraying apparatus, equipped with a variable high-voltage 0-
204 30 kV power supply. The emulsions were introduced in a 5 mL plastic syringe
205 and were pumped at a flow-rate of 0.15 mL/h through a stainless-steel needle (0.9 mm
206 of inner diameter). The needle was connected through a PTFE wire to the syringe,
207 which was placed on a digitally controlled syringe pump. Processed samples were
208 collected on a stainless-steel plate connected to the cathode of the power supply and
209 placed facing the syringe in a horizontal configuration, at a distance of 10 cm. The
210 applied voltage was 15 kV for the gelatin emulsions and 17 kV for SPI and WPC
211 emulsions. The above processing parameters were selected from preliminary tests in
212 order to attain stable electrospraying, avoiding dripping of the solution.

213

214 **2.7. Morphological characterization of the particles**

215 Scanning electron microscopy (SEM) was conducted on a Hitachi microscope (Hitachi
216 S-4800) at an accelerating voltage of 10 kV and a working distance of 8-9 mm. Samples
217 were sputter-coated with a gold-palladium mixture under vacuum prior to examination.
218 Particle diameters were measured from the SEM micrographs in their original
219 magnification using the ImageJ software. Size distributions were obtained from a
220 minimum of 200 measurements.

221

222 **2.8. Fourier transform infrared (FT-IR) analysis of the samples**

223 FT-IR spectra were collected in transmission mode using a Bruker (Rheinstetten,
224 Germany) FT-IR Tensor 37 equipment following the methodology described in Gómez-
225 Mascaraque et al. (2015).

226

227 **2.9. Microencapsulation efficiency**

228 The microencapsulation efficiency (MEE) of the ALA-loaded capsules was determined
229 based on FT-IR absorbance measurements. A calibration curve was obtained for each
230 encapsulation matrix (R_{Gel}^2 = 0.999, R_{SPI}^2 = 0.993, R_{WPC}^2 = 0.986) from the spectra of
231 protein/ALA mixtures of known relative concentrations (0, 5, 10 and 15 % w/w of
232 ALA). The relative absorbance intensities of the peaks at 3012-3013 cm^{-1} (attributed to
233 ALA) and at 1541-1543 cm^{-1} (corresponding to the Amide II band of the proteins) were
234 plotted against the ALA concentration in the mixtures. The intact ALA content in the
235 capsules was interpolated from the obtained linear calibration equations. The MEE of
236 the ALA-loaded particles was then calculated using Eq. (2):

237 $$MEE\ (\%) = \frac{Content\ of\ ALA\ in\ the\ capsules}{Content\ of\ ALA\ initially\ added\ to\ the\ emulsions} \times 100 \qquad \text{Eq. (2)}$$

238

239 **2.10. Thermal Properties of the materials**

240 Thermogravimetric analysis (TGA) was performed with a TA Instruments model Q500
241 TGA. The samples (ca. 8 mg) were heated from 25ºC to 600ºC with a heating rate of

10ºC/min under dynamic air atmosphere. Derivative TG curves (DTG) express the weight loss rate as a function of temperature.

2.11. Accelerated oxidation assays for free and microencapsulated ALA

Non-encapsulated and microencapsulated ALA was subjected to thermal treatment at 80°C in order to evaluate the protective effect of each wall material. After selected time intervals, FT-IR spectra were recorded for each sample, and the absorbance intensity of the band at 3012-3013 cm^{-1}, corresponding to ALA, was measured. The decrease in the relative intensity of the aforementioned band was related to the extent of degradation of ALA within the capsules or in its native form, as previously reported (Torres-Giner, Martinez-Abad, Ocio, & Lagaron, 2010).

2.12. Statistical analysis

A statistical analysis of experimental data was performed using IBM SPSS Statistics software (v.23) (IBM Corp., USA). Significant differences between homogeneous sample groups were obtained through two-sided t-tests (means test of equality) at the 95% significance level ($p < 0.05$). For multiple comparisons, the p-values were adjusted using the Bonferroni correction.

3. Results and discussion

3.1. Characterization of O/W emulsions

263 Two different procedures were used for the preparation of the emulsions, as illustrated
264 in Figure 1. The first approach consisted of a simple high-speed homogenization
265 treatment, while the second one included a second ultrasonication step aimed at
266 reducing the droplet size of the emulsions (Leong, Wooster, Kentish, & Ashokkumar,
267 2009). In general, smaller droplets lead to increased stability of emulsions and improved
268 bioavailability of the active ingredients (McClements, 2011, 2012), also facilitating
269 their inclusion and dispersion within the fine microencapsulation structures to be
270 produced. However, ultrasonic treatments may heat the emulsions, potentially leading to
271 partial degradation of thermosensitive bioactives. Therefore, both approaches were used
272 for the preparation of the emulsions and the impact of the ultrasonication treatment was
273 studied. Figure 2 shows the images obtained by optical microscopy for the different
274 emulsions produced using SBO as a model oily phase.

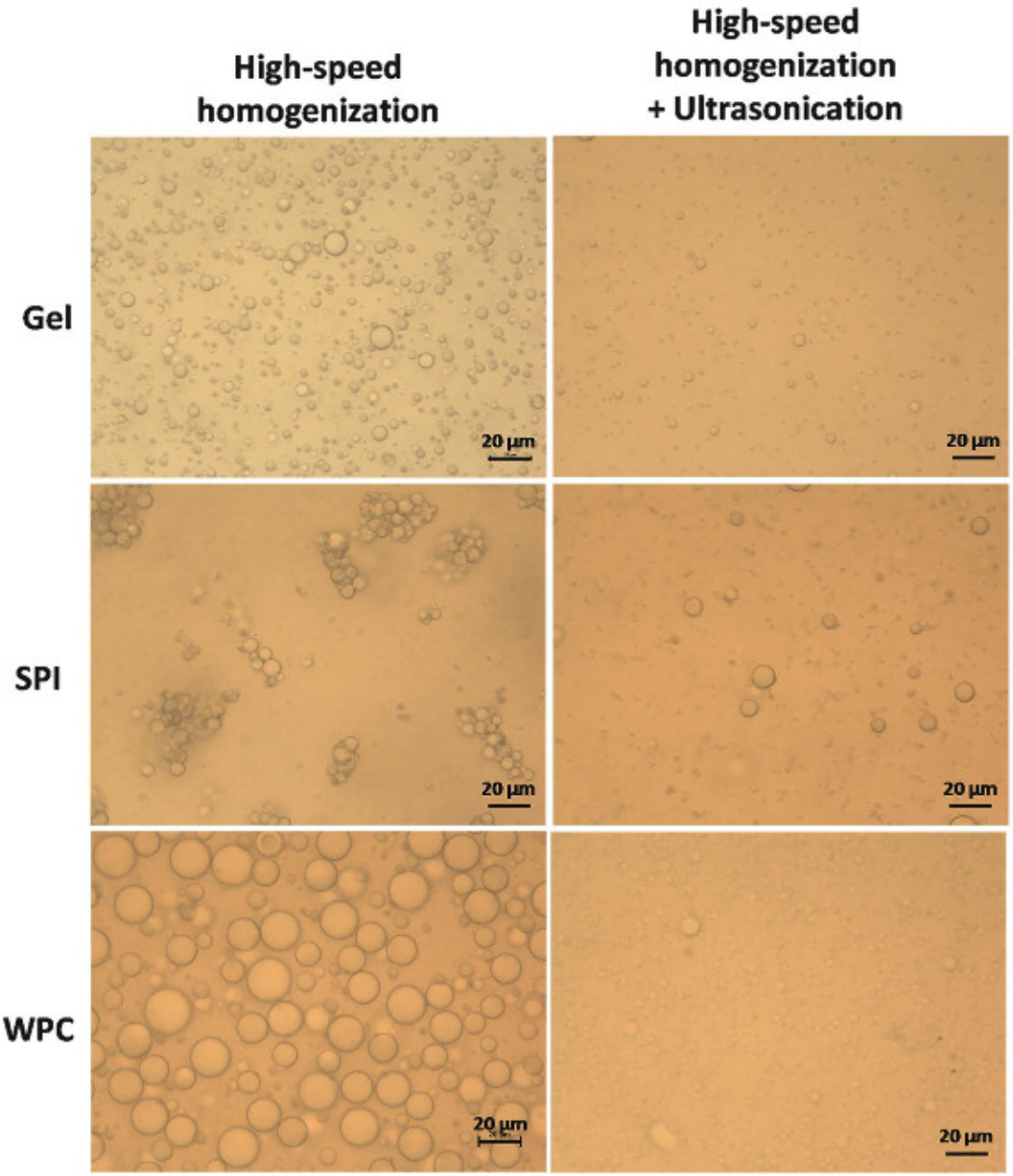

Figure 2. Optical micrographs for the different emulsions produced using SBO. Scale bars represent 20 µm

The appearance of the emulsions produced using the first approach (single high-speed homogenization step) was dramatically different for each protein. Gel and WPC led to well dispersed droplets, which were significantly smaller for Gel, while flocculated droplets were observed for SPI emulsions. These differences were also manifested in their rheological behaviour, i.e. while the emulsions prepared using Gel and WPC exhibited quite a Newtonian behaviour in the range of study, the emulsion prepared in

285 the single high-speed homogenization step using SPI showed a manifest shear thinning
286 behaviour (cf. Figure S1 of the Supplementary Material), usually associated to a high
287 degree of droplet flocculation (McClements, 2007; Surh et al., 2006). This strong shear
288 thinning behaviour, together with the high viscosity of the emulsion suggested that the
289 mechanism of flocs formation was by bridging flocculation, which occurs when the
290 protein chains or aggregates are shared between two droplets (Malaki Nik, Wright, &
291 Corredig, 2010). A plausible explanation for the occurrence of bridging flocculation
292 when using SPI involves the previous denaturation step which is carried out for this
293 protein as a requirement for the subsequent electrospraying process (Pérez-Masiá et al.,
294 2014). Denaturation leads to protein unfolding and thus to increased exposure of its
295 non-polar amino acids. This may promote droplet flocculation in oil-in-water emulsions
296 through increased hydrophobic attraction between protein chains adsorbed onto
297 different droplets (McClements, 2004).

298

299 When the second emulsification approach was applied (i.e. including an ultrasonication
300 treatment) the droplet size was indeed greatly reduced for the three protein formulations
301 tested. Moreover, the SPI-stabilized emulsion turned Newtonian, with a substantial
302 decrease in its viscosity, suggesting that the flocs were disrupted. Previous studies had
303 shown a decrease in the extent of droplet aggregation and apparent viscosity upon
304 ultrasound treatments, in addition to a reduction of the mean particle size (Surh et al.,
305 2006).

306

307 **3.2. Creaming stability of the emulsions**

The creaming index of an emulsion after a particular time lapse is an indicative of its stability to gravitational separation. As the density of the oil droplets in an O/W emulsion is lower than that of its aqueous environment, they tend to move upwards unless efficiently stabilized (McClements, 2007). The creaming index (CI) of the emulsions prepared in this work after 5, 24 and 48 h are summarized in Table 1, and the appearance of the emulsions with or without a cream layer is shown in Figure S2 of the Supplementary Material.

Table 1. Creaming index (CI) of the emulsions, calculated according to Eq. 1

Emulsion		5 h	24 h	48 h
Protein	**Emulsion procedure**			
Gel	HSH	0%	0%	1%
Gel	HSH+US	0%	0%	0%
SPI	HSH	4%	4%	4%
SPI	HSH+US	0%	0%	0%
WPC	HSH	0%	24%	15%
WPC	HSH+US	0%	13%	9%

Five hours after preparation the SPI emulsion prepared through high-speed homogenization (without ultrasound treatment) already experienced creaming, which was not surprising taking into account the presence of big flocs in this sample (cf. Figure 2). The rest of the emulsions did not show signs of gravitational separation during these first 5 hours, meaning that they were stable to creaming during at least the time required to electrospray them. Gelatin was the most efficient protein system evaluated for the stabilization against gravitational separation of the emulsions, only experiencing subtle creaming after 48 h when no ultrasound treatment was applied, due to the bigger droplet sizes. On the other hand, sonication had a positive effect on the stability of SPI-based emulsions, as the disruption of the flocs together with the droplet

size reduction avoided the creaming phenomenon during at least 48 h. Regarding WPC, a thick cream layer appeared after 24 h, which further compacted during the following day reaching smaller CIs at 48 h. This cream layer was obviously thicker for the non-sonicated emulsion, due to its considerably bigger droplet size. Thick cream layers are usually caused by bridging flocculation, as strong attractive forces yield less packed flocs (McClements, 2007). However, unlike the SPI emulsion produced through procedure 1, WPC emulsions did not show signs of flocculation during the first hours after preparation. The reason for this late flocculation might be related to the conformational changes that globular proteins may suffer resulting from adsorption to an interface (McClements, 2004), consequently exposing their non-polar and cysteine residues to the aqueous phase. This phenomenon has been described for whey proteins, where disulphide cross-linking can occur at the interface (Malaki Nik et al., 2010). In SPI, as denaturation was forced through the previous thermal treatment, a much earlier flocculation was observed until the emulsion was ultrasonicated. Conversely, the ultrasound treatment in the WPC-stabilized emulsion was applied before the addition of the protein, so it could not affect its reassembling.

3.3. Morphology of electrosprayed capsules from O/W emulsions

The production of microcapsules from protein-stabilized emulsions by spray-drying has been studied in a number of works. However, the emulsion electrospraying approach has only recently been proposed for the microencapsulation of functional ingredients (Pérez-Masiá et al., 2015). Thus, in order to ascertain the feasibility of producing electrosprayed microencapsulation structures from the prepared emulsions (i.e. using

SBO as a model oil), these were subjected to hydrodynamic processing (cf. Section 2.6. for process parameters) and the obtained structures are shown in Figure 3.

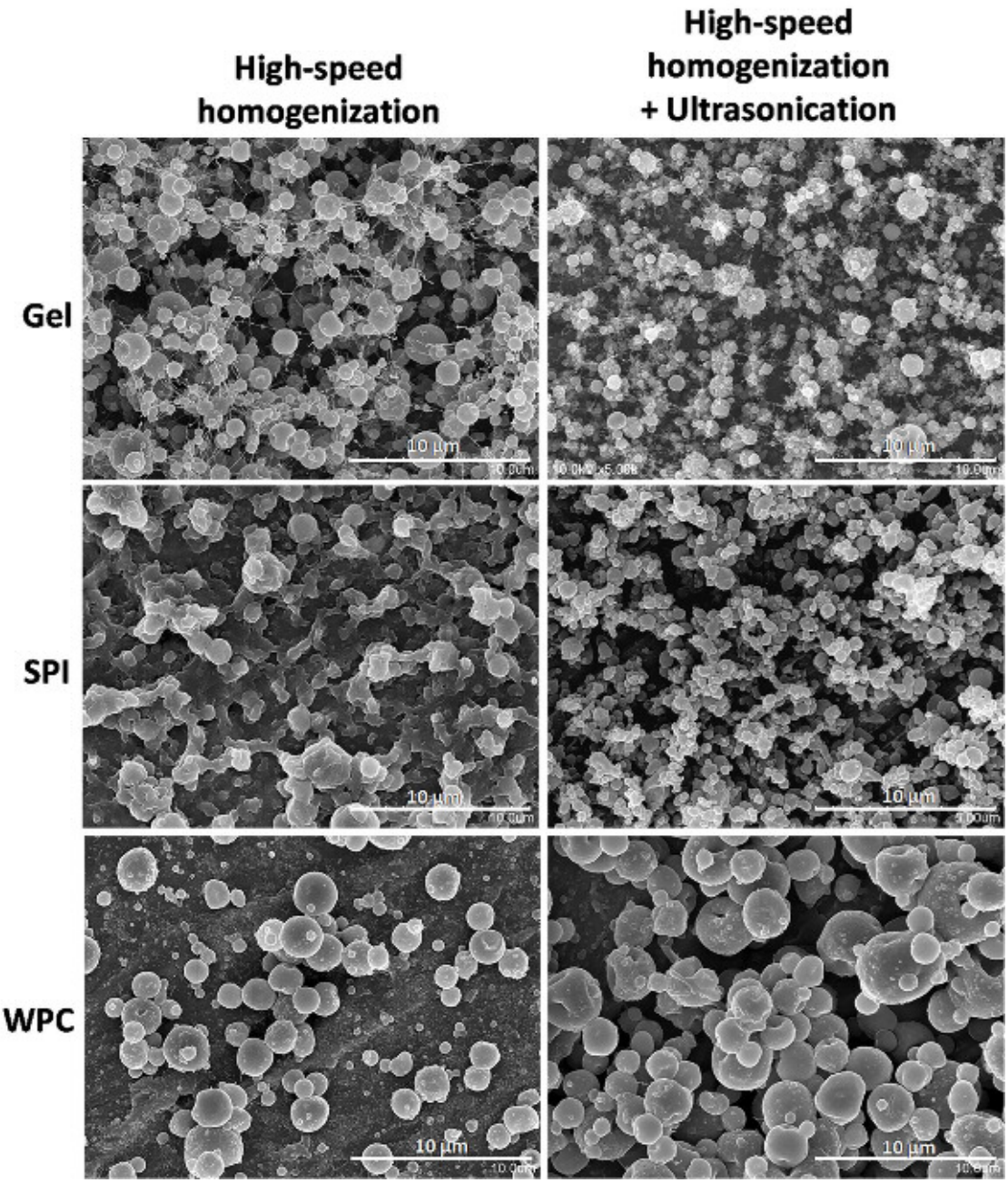

Figure 3. SEM images of electrosprayed structures obtained from the protein-stabilized SBO/W emulsions prepared using Procedure 1 (left) and Procedure 2 (right). Scale bars correspond to 10 µm.

From the micrographs it was concluded that gelatin was the only protein which yielded proper microparticulate structures when the first emulsification procedure was used. The structure obtained using SPI showed signs of dripping and wetted particles while WPC yielded a mixed structure exhibiting a continuous polymeric surface below some

360 spherical microcapsules. This can be explained in the light of the properties and droplet
361 size distribution of each emulsion. While gelatin exhibited the smallest droplet sizes
362 using Procedure 1 (cf. Figure 2), SPI emulsion formed large floccules and the size the
363 majority of the droplets in the WPC emulsion was too big to be encapsulated within the
364 generated smaller microcapsules. Although the effective volume of the droplet is
365 significantly increased by the absorbed proteins on their surface (Howe & Pitt, 2008;
366 Malaki Nik et al., 2010), which means that the actual oil volume is smaller than the
367 apparent droplet size, some of the droplets in WPC and the floccules in SPI were still
368 too big for microcapsule formation.

369 Upon ultrasound treatment, the droplet size was dramatically reduced for the three
370 protein systems, so that all of them could yield neat microcapsules when electrosprayed,
371 even though the particle size also decreased (except for WPC). The size and
372 morphology of these particles varied from one protein to another, and this can be
373 attributed not only to the characteristics of the emulsion droplets but also to the
374 properties of the proteins themselves. WPC dispersions in the absence of added oils or
375 bioactive compounds usually give rise to bigger particles than gelatin or SPI (Gómez-
376 Mascaraque et al., 2015; Pérez-Masiá et al., 2014) for similar concentrations and
377 electrospraying conditions as the ones used in this work.

378

379 **3.4. Morphology of ALA-loaded electrosprayed and spray-dried capsules**

380 Once the feasibility of the emulsion electrospraying technique had been confirmed for
381 the three proteins, the model SBO was substituted by the bioactive ω-3 fatty acid, ALA.
382 The emulsions were prepared using the second procedure, including the ultrasound
383 treatment, as it proved to be more adequate for the encapsulation of oil droplets in the

previous section, and they were processed both by electrospraying and spray-drying. Emulsions prepared using Procedure 1 were also electrosprayed for comparison purposes. Figure 4 shows the micrographs of the obtained structures and Figure S3 of the Supplementary Material summarizes the particle size distribution for each sample.

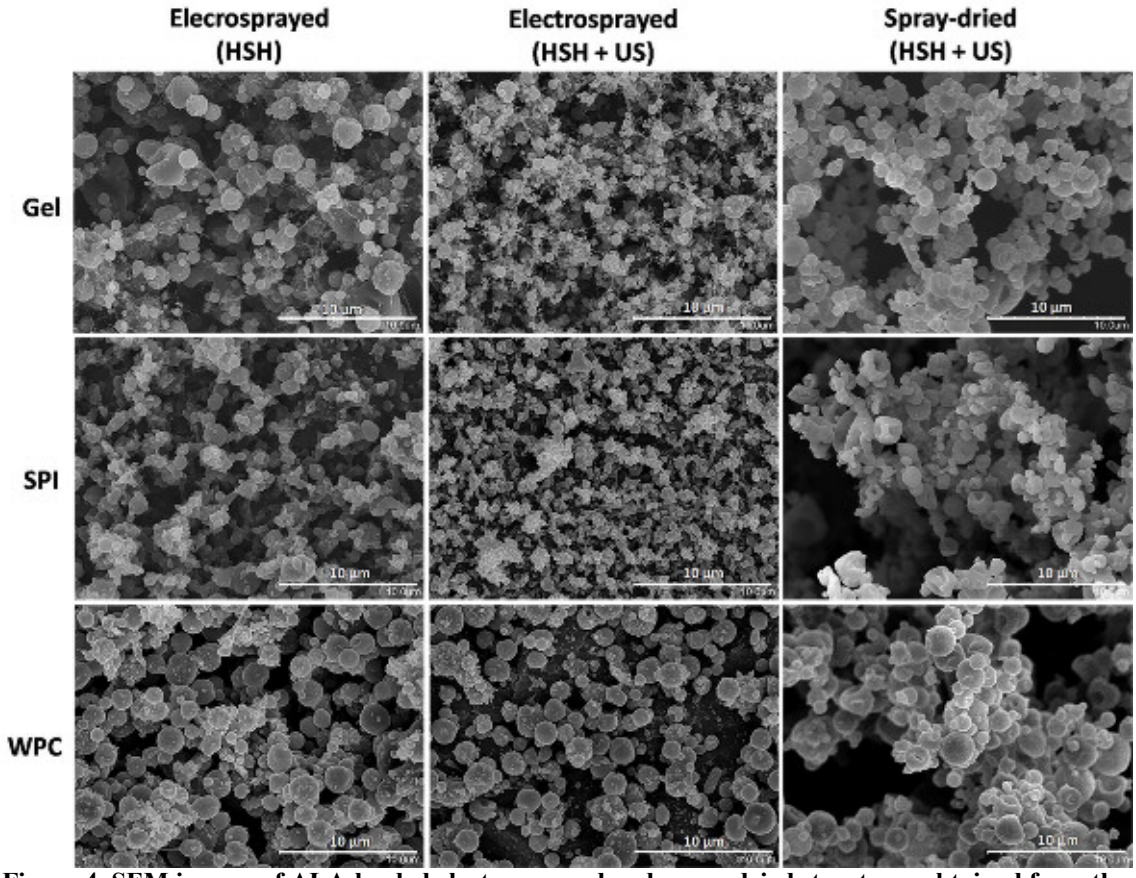

Figure 4. SEM images of ALA-loaded electrosprayed and spray-dried structures obtained from the protein-stabilized emulsions. Scale bars correspond to 10 µm.

Surprisingly, both the emulsions prepared through Procedures 1 and 2 allowed the production of micro- or submicroparticles through electrospraying. These results suggest smaller droplet sizes of the emulsions prepared with ALA in comparison with the ones prepared using the model oil, SBO. In fact, although ALA is water insoluble, it has a polar head in its structure which provides enhanced compatibility through reorganization of the lipid molecules to expose their carboxyl groups to the water interface, fact which can contribute to increased stability of the emulsions and decreased

399 droplet size. Also, the extent of protein unfolding at the interface is usually larger for
400 more non-polar oils (McClements, 2004), so the flocculation of the emulsions prepared
401 with the globular proteins might have been prevented. As a result, the six emulsions
402 yielded ALA-loaded microencapsulation structures through electrospraying.

403 In general, the ultrasonicated emulsions led to smaller particle size distributions, with
404 the exception of WPC, where little differences in the particle diameters were observed.
405 This can be attributed to the increase in surface tension and electrical conductivity
406 (Jaworek & Sobczyk, 2008) found after the ultrasound treatment (cf. Section 2.1.3.),
407 and also to their expected smaller droplet sizes, The structures obtained through spray-
408 drying showed bigger mean diameters than the ones obtained through electrospraying,
409 as observed in previous works (Pérez-Masiá et al., 2015).

410

411 **3.5. Molecular organization**

412 FTIR spectroscopy was used to characterize the molecular organization of the
413 microencapsulation structures. For this purpose, the spectra of emulsion electrosprayed
414 and spray-dried ALA-loaded particles were compared to those of the raw proteins and
415 the free fatty acid. The spectra of the unloaded particles were also obtained.

416 The IR spectrum of commercial ALA showed its most representative bands centered at
417 3013 cm^{-1} (stretching of *cis*-alkene groups -HC=CH- in PUFAs) and 1711 cm^{-1} (C=O
418 stretching in fatty acids) (Moomand & Lim, 2014). Other relevant bands of the
419 bioactive compound were found at 2965, 2932 and 2856 cm^{-1} due to the methyl
420 asymmetrical stretching, the methylene asymmetrical stretching and the methylene
421 symmetrical stretching vibrations, respectively (Guillen & Cabo, 1997). On the other
422 hand, the spectra of the three as-received proteins showed the characteristic bands

423 ascribed to the vibration of the bonds in their amide groups, referred as the Amide A
424 (N-H stretching), Amide B (asymmetric stretching vibration of =C-H and $-NH_3^+$),
425 Amide I (C=O stretching), Amide II (N-H bending and stretching) and Amide III (C-N
426 stretching) bands (Aewsiri, Benjakul, Visessanguan, Wierenga, & Gruppen, 2010;
427 Nagarajan, Benjakul, Prodpran, Songtipya, & Nuthong, 2013). Also noticeable are the
428 bands observed around 2960 cm^{-1} and 2930 cm^{-1}, corresponding to the $-CH_2$ asymmetric
429 and symmetric stretching vibrations, respectively (Nagiah, Madhavi, Anitha, Srinivasan,
430 & Sivagnanam, 2013).

431 Regarding the microencapsulation structures, differences in their characteristic bands
432 were observed in comparison with the as-received proteins. Table 2 shows a summary
433 of the wavenumbers at which each of these characteristic bands were found, and the
434 complete spectra are provided as supplementary data (cf. Figure S4). Interestingly,
435 ALA-loaded particles produced using different emulsification protocols (i.e. with or
436 without the ultrasonication step) yielded similar infrared spectra, only differing in the
437 intensity of the peak at 3013 cm^{-1}, due to the presence of ALA. Thus, for simplification
438 purposes only the results for the materials obtained following the first emulsification
439 approach are displayed. The spectral data of unloaded electrosprayed particles are also
440 provided.

441

442 **Table 2. Characteristic FTIR absorption bands (wavelengths in cm^{-1}) of as-received proteins and microencapsulation structures thereof**

	Gel (raw)	Gel ES (unloaded)	ALA-loaded Gel ES	ALA-loaded Gel SD	SPI (raw)	SPI ES (unloaded)	ALA-loaded SPI ES	ALA-loaded SPI SD	WPC (raw)	WPC ES (unloaded)	ALA-loaded WPC ES	ALA-loaded WPC SD
Amide A	3430	3312	3313	3313	3294	3289	3289	3289	3297	3293	3293	3293
Amide B	3085	3080	3080	3080	3075	3075	3075	3075	3078	3078	3077	3079
Amide I	1642	1653	1653	1653	1653	1653	1653	1655	1651	1654	1654	1654
Amide II	1543	1541	1541	1541	1534	1542	1543	1543	1540	1540	1543	1543
Amide III	1244	1244	1244	1244	1240	1251	1250	1250	1262	1249	1248	1248
-CH2	2960, 2928	2961, 2939	2961, 2931	2961, 2938	2961, 2928	2956, 2925	2957, 2927	2957, 2927	2963, 2924	2959, 2927	2959, 2927	2958, 2926
ALA	-	-	3013	-	-	-	3012	-	-	-	3013	-

443 ES = Electrosprayed; SD = Spray-dried

444 After processing the proteins, both by emulsion electrospraying and spray-drying, a
445 general narrowing of the peaks was observed, which has already been described in
446 previous works (Gómez-Mascaraque et al., 2015; López-Rubio & Lagaron, 2012).
447 Moreover, the Amide A band shifted to significantly lower wavenumbers for the three
448 proteins, indicating changes in the hydrogen bonding structure of the proteins (Doyle,
449 Bendit, & Blout, 1975). These changes have been previously attributed to the removal
450 of the structural water during the rapid drying process in the formation of electrosprayed
451 gelatin particles (Gómez-Mascaraque et al., 2015), and this hypothesis could be
452 extended to the other proteins as inferred from the TGA analysis (see below). The
453 Amide B band only experienced a displacement towards lower wavenumbers for
454 gelatin, not being significantly affected upon processing of SPI or WPC. This is
455 attributed to the processing conditions of gelatin in diluted acetic acid and subsequent
456 protonation of its amino groups, being this band partially due to the vibration of $-NH_3^+$
457 groups. Gelatin also showed the most significant changes in the displacement of the
458 Amide I band upon processing, which is attributed to changes in the secondary structure
459 of proteins (Ebrahimgol, Tavanai, Alihosseini, & Khayamian, 2014). Although the
460 denaturation of SPI prior to processing did not lead to displacements in the Amide I
461 band, which only narrowed, it did have an impact on the Amide II band, which is also
462 conformationally sensitive (Aceituno-Medina, Mendoza, Lagaron, & López-Rubio,
463 2013; Long et al., 2015)), producing a considerable shift towards higher wavenumbers,
464 as previously observed (Pérez-Masiá et al., 2014). The Amide III band also experienced
465 changes in its shape for both WPC and SPI, but not for gelatin, although the complex
466 mixture of globular proteins present in these samples limits the interpretation of these
467 results. Finally, the relative intensities of the bands corresponding to the asymmetric
468 and symmetric stretching vibrations of methylene groups and their peak maxima

469 changed upon processing of the proteins, especially for SPI and WPC (which contained
470 the surfactant). It is worth noting that these general comments are valid for both
471 electrosprayed and spray-dried capsules, which exhibited little differences between
472 them in terms of the bands ascribed to the proteins.

473 The presence of the ω-3 fatty acid in the electrosprayed encapsulation microstructures
474 was evidenced by the existence of its characteristic absorption band at 3013 cm^{-1} in
475 these samples. However, this peak was not detected for any of the spray-dried materials,
476 suggesting that the bioactive compound was completely degraded during processing
477 through the latter technique, due to the high temperatures required for the production of
478 the encapsulation structures in this case. As the aforementioned band is related to the
479 presence of *cis*-alkene groups in the samples, its disappearance implies that these double
480 bonds were no longer present in the samples, i.e. they had been oxidized. Therefore,
481 regardless of the protein used as wall material, electrospraying proved to be an effective
482 technique for the microencapsulation of the thermosensitive bioactive while spray-
483 drying resulted in complete ALA degradation. Other works had reported the successful
484 encapsulation of ALA-rich oils, such as linseed oil (Gallardo et al., 2013) or chia oil
485 (Rodea-González et al., 2012), within proteins and polyssacharides through spray-
486 drying. However, pure ALA (>99%) showed extreme sensitivity to heat and thus it
487 could not be detected in any of the spray-dried samples. Therefore, only the
488 electrosprayed capsules will be considered in the following sections.

489

490 **3.6. Microencapsulation efficiency**

491 The band at 3013 cm^{-1} was also used to estimate the microencapsulation efficiency
492 (MEE) for the electrosprayed materials, as it did not overlap with any of the bands of

493 the proteins and it was a good indicator for the integrity of the bioactive compound.
494 Hence, the MEE estimated in this work is based on the presence of intact double bonds
495 in the bioactive fatty acid rather than the mere content of oil (oxidized or not) which is
496 measured in other works by gravimetric techniques (Jiménez-Martín, Gharsallaoui,
497 Pérez-Palacios, Carrascal, & Rojas, 2014; Rodea-González et al., 2012; Wang,
498 Adhikari, & Barrow, 2014). Calibration curves were constructed for each ALA-protein
499 system (R^2_{Gel} = 0.999, R^2_{SPI} = 0.993 and R^2_{WPC} = 0.986) using physical mixtures of the
500 unloaded electrosprayed proteins with known relative concentrations of the fatty acid,
501 and using the Amide II band of each protein as a reference. The MEE of the ALA-
502 loaded particles was then calculated using Eq. (2) and the results are summarized in
503 Table 3.

504 **Table 3. Microencapsulation efficiencies for the electrosprayed materials. Different letters (a-e)**
505 **within the same column indicate significant differences at p < 0.05 among the samples**

Electrosprayed sample		
Protein	**Emulsion procedure**	**MEE (%)**
Gel	HSH	40 ± 4 [a,c]
Gel	HSH+US	23 ± 12 [a]
SPI	HSH	61 ± 4 [b]
SPI	HSH+US	30 ± 3 [a]
WPC	HSH	67 ± 5 [b]
WPC	HSH+US	50 ± 3 [b,c]

506 **HSH = High-speed homogeneization; US = Ultrasonication**

507
508 In general, the estimated MEE was considerably higher when no ultrasound was used
509 for emulsion preparation. This was directly related to the heating of the emulsions
510 during the ultrasonication treatment, which must have partially degraded the
511 thermosensitive fatty acid. In fact, despite the short duration (i.e. 30 s) of the treatment
512 intervals and the use of an ice bath to cool down the samples, the temperature of the

emulsions after de ultrasonication treatment raised up to 45 ºC. Hence, although the second emulsification approach proved to be useful to decrease de droplet size of the emulsions and increase their stability, it caused partial oxidation of the bioactive oil before encapsulation.

Concerning the MEE of the different proteins, gelatin yielded the lowest values regardless of the emulsification protocol employed. This was attributed to the low pH of the gelatin solution prepared in diluted acetic acid, which might have contributed to the greater degradation of the fatty acid before and during processing. Recent studies also found greater extents of lipid oxidation in ALA-containing SBO at acidic pH than at neutral pH (Kapchie, Yao, Hauck, Wang, & Murphy, 2013), supporting this hypothesis.

The best results were achieved when either SPI or WPC were used as wall matrices and the first and simplest emulsification approach was employed, both samples belonging to the same statistical group (cf. Table 3). Remarkably, those two emulsions were the most unstable when SBO was used as a model oil, even leading to bridging flocculation. However, the differences in the model oil and the bioactive oil structures might have led to improved stability of the latter, as commented above.

3.7. Thermogravimetric analysis of the materials

Thermogravimetric analysis of the raw proteins and the free ALA, as well as the unloaded and ALA-loaded electrosprayed particles, was conducted in oxidative conditions at 10ºC/min in order to assess potential thermostability changes of the bioactive ingredient upon microencapsulation. A physical mixture of the unloaded electrosprayed materials and ALA (10% w/w) was also analysed. Figure 5 shows the obtained DTG curves.

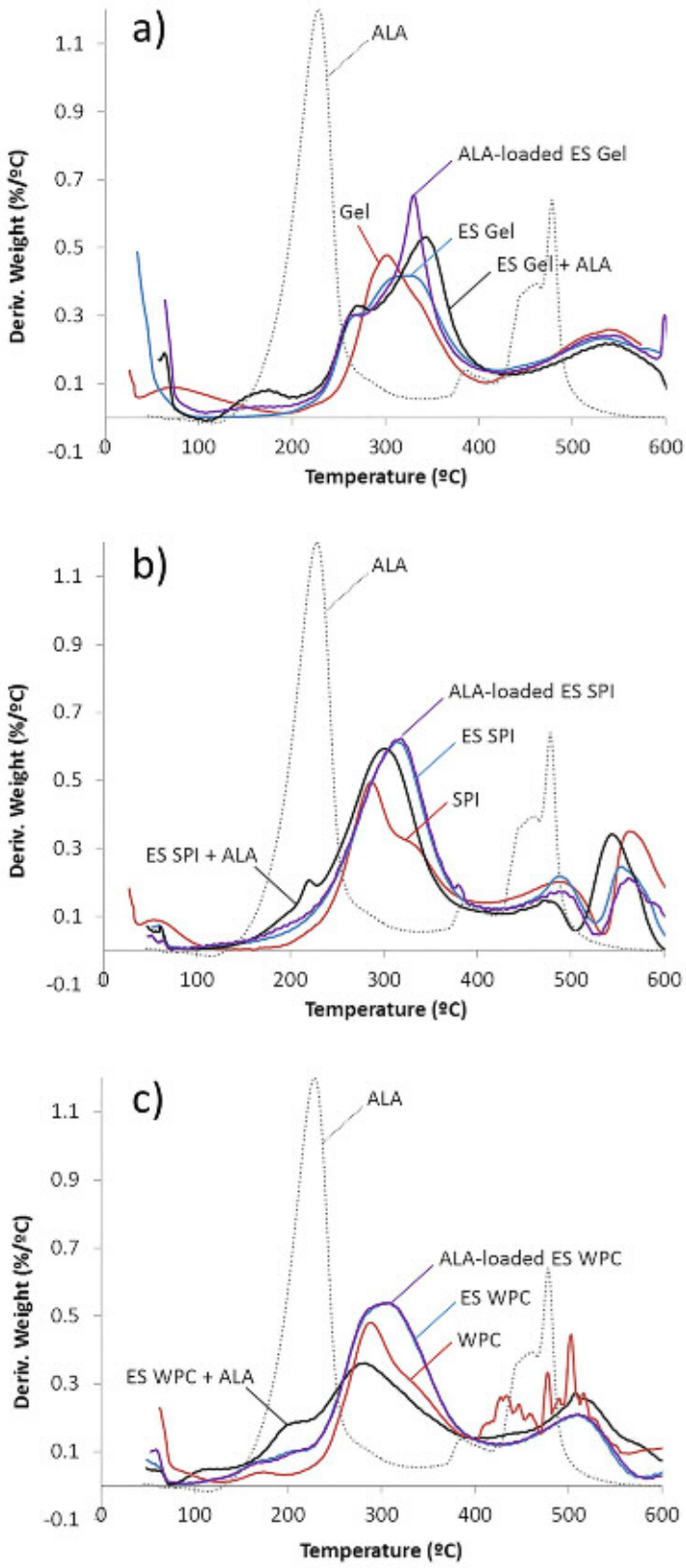

Figure 5. DTG curves of raw ALA, as-received proteins, e-sprayed particles and their mixtures for gelatin (a), SPI (b) and WPC (c).

541 The main degradation stage (major weight loss) for free ALA had its temperature of
542 maximum degradation rate (T_{max}) at 228 ºC. In contrast, the main degradation stage for
543 the three proteins took place in the range of 250-400ºC for all the materials. Thus, the
544 degradation of both components could be distinguished in the physical mixtures. For
545 instance, a small peak at T_{max}=219 ºC was observed for SPI and a small shoulder at
546 T_{max}=215 ºC for WPC, which were both attributed to the presence of ALA, as they were
547 not present in the unloaded electrosprayed proteins alone. The decrease in the thermal
548 stability of ALA in these mixtures could be attributed to its increased exposed surface
549 when physically absorbed on the proteins. For gelatin, its physical mixture with the fatty
550 acid exhibited a small weight loss well below the T_{max} of the free bioactive, which was
551 absent in the neat electrosprayed gelatin, and hence was similarly attributed to the
552 degradation of free ALA absorbed on the gelatin surface. The exceptional decrease in
553 stability in this case could be motivated by the presence of residual acetic acid in the
554 capsules.

555 The DTG curves of the ALA-loaded encapsulation structures showed similar
556 degradation profiles to those of the unloaded particles. Both exhibited slight changes in
557 the degradation profile of the main stage when compared to the as-received proteins. As
558 previously reported for gelatin (Gómez-Mascaraque et al., 2015), the T_{max} of the main
559 degradation stage of the three protein systems increased upon electrospraying, although
560 the onset temperature decreased (i.e. the degradation started at lower temperatures).
561 These changes have been attributed to the structural changes caused by the
562 electrospraying process and the reduction of the particle size, which results in an
563 increase of the specific area and, consequently, of their susceptibility to thermal
564 degradation (Gómez-Mascaraque et al., 2015). Regardless, the weight losses attributed
565 to ALA in the mixtures were not found in the ALA-containing encapsulation structures,

566 suggesting an increase in the thermal stability of the bioactive fatty acid upon
567 encapsulation, as its degradation was delayed until its protective matrices themselves
568 degraded.

569 Another interesting feature, also observed in previous works dealing with
570 electrospraying of proteins (Gómez-Mascaraque et al., 2015), is that their fast drying
571 triggered the removal of their structural water, so that only losses of absorbed water
572 were afterwards detected in the processed materials (up to 100ºC), while the as-received
573 proteins prolonged the weight loss attributed to solvent (water) evaporation up to
574 around 125ºC in SPI and WPC and even close to 200ºC for gelatin. This would have an
575 impact on the structural changes detected by infrared spectroscopy.
576

577 **3.8. Accelerated oxidation/degradation assays**

578 The protective effect of the different emulsion electrosprayed encapsulation structures
579 on the oxidative stability of ALA was assessed through an accelerated degradation assay
580 at 80ºC. For this purpose, the relative intensity of the infrared band attributed to the
581 presence of alkene groups (3012-3013 cm^{-1}) was measured after different time periods
582 at this temperature. The decrease in the relative absorbance of this band was related to
583 the extent of ALA degradation (Torres-Giner et al., 2010). Results were normalized to
584 the initial ALA content in the capsules for a better comparison of the different matrices,
585 and they are shown in Figure 6.

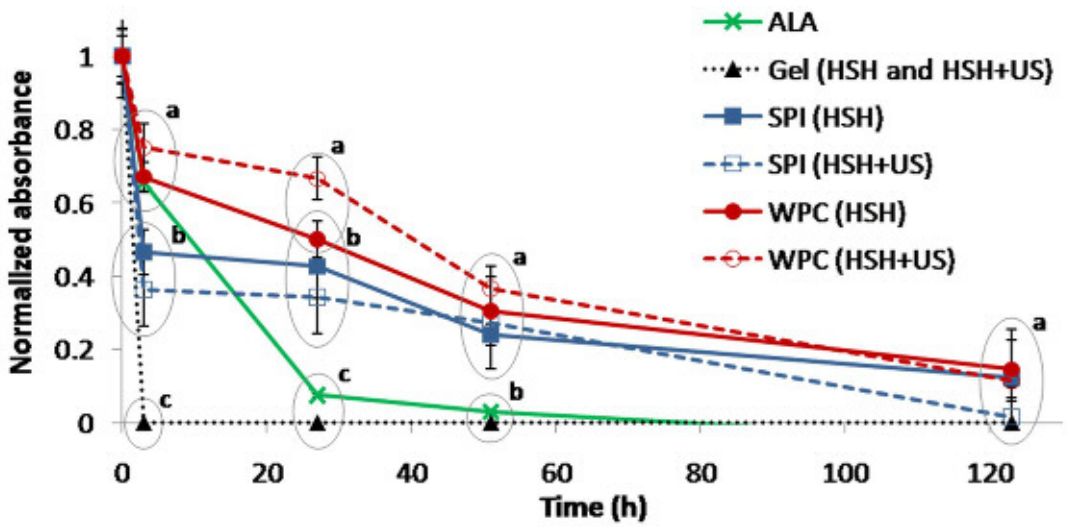

586
587 **Figure 6. Degradation profiles at 80ºC for free and encapsulated ALA. Different letters (a-c) within**
588 **the same time period indicate different statistical groups with significant differences among them at**
589 **$p < 0.05$**

590

591 The peak of interest was not detected in any of the gelatin samples after only 3 hours of
592 thermal treatment, emphasizing that not only this matrix did not protect ALA from
593 thermal oxidation, but it also accelerated its degradation, most probably due to the
594 presence of residual acetic acid in the capsules.

595 Regarding the globular proteins, the degradation of ALA within the WPC matrices did
596 not show significant differences with that of free ALA during the first 3 h, although the
597 stability of the encapsulated fatty acid was significantly improved during the following
598 days. This fast, initial degradation could be attributed to the fraction of the bioactive
599 allocated on the surface or very close to the surface of the particles.

600 A similar degradation profile was found for ALA-loaded SPI capsules. However, in this
601 case during the first hours of high temperature exposure, a greater extent of degradation
602 was observed in comparison with that of free ALA. This might be attributed to the
603 increased specific area of the ALA domains located on the surface of the particles.
604 Compared to free ALA in bulk, whose specific area exposed to air was low, the

605 encapsulated fatty acid was fragmented into very small domains (droplets) by
606 emulsification prior to electrospraying, greatly increasing its specific area. Thus, if a
607 fraction of this oil remained on the surface of the particles, it would be more exposed to
608 the environment. This statement would also be applicable to WPC, meaning that the
609 fraction of oil on the surface of the protein particles would be lower for the WPC than
610 for SPI. This difference could be attributed, among other factors, to the bigger particle
611 sizes of the WPC capsules, which thus had smaller specific surface area. After the first
612 three hours, the degradation of encapsulated ALA, both within SPI and WPC particles,
613 was significantly delayed with respect to free ALA, highlighting the effective protection
614 of these electrosprayed matrices against oxidation at high temperatures.

615 While the protection exerted by the WPC capsules was enhanced compared to the SPI
616 particles during the first hours of treatment, no significant differences were observed
617 among the samples after 2 days. Furthermore, the procedure used for the preparation of
618 the emulsions had little effect on the degradation profiles, despite its impact on the
619 encapsulation efficiency. Only WPC showed a significant difference between both
620 methodologies after the first 27 hours of treatment, most probably due to the bigger
621 droplet sizes of the non-ultrasonicated emulsion, which led to a bigger fraction of non-
622 encapsulated or superficial oil, taking into account that the particle size of the capsules
623 was very similar for both approaches.

624

625 **4. Conclusions**

626 A novel emulsion electrospraying technique has been used to develop protein-based
627 microencapsulation structures for the protection of ALA (used as a model
628 thermosensitive hydrophobic bioactive compound) and compared with a well-

established technology used in the food industry such as spray-drying. Being ALA a thermosensitive compound, spray-drying was inappropriate for this purpose, completely degrading the ω-3 fatty acid. As hypothesised, the electrospraying technique proved to be a satisfactory alternative, achieving microencapsulation efficiencies of up to 67% ± 5%. It was also found that the low pH required for processing gelatin through electropraying resulted in quick degradation of the encapsulated bioactive, while the ultrasound treatment for emulsion preparation also decreased the MEE due to heating. Thus, the best results were achieved using the globular proteins (WPC and SPI) and the simple homogenization procedure for the preparation of the emulsions, significantly delaying ALA oxidation during accelerated degradation assays at 80ºC. The overall results of the present work demonstrate the potential of electrospraying of protein-stabilized emulsions for the microencapsulation and enhanced protection of thermosensitive and hydrophobic bioactive ingredients, specifically ω-3 fatty acids, offering an improved alternative to traditional technologies used in the food industry such as spray-drying, which gives rise to oxidative degradation and does not significantly protect ω-3 fatty acids (Kolanowski, Ziolkowski, Weißbrodt, Kunz, & Laufenberg, 2006). Further research will be needed to extend the applicability of these results to a wider range of hydrophobic bioactive ingredients and wall materials.

Acknowledgements

Laura G. Gómez-Mascaraque is recipient of a predoctoral contract from the Spanish Ministry of Economy and Competitiveness (MINECO), Call 2013. The authors would like to thank the Spanish MINECO project AGL2012-30647 for financial support. Sara Díaz Cuesta is also acknowledged for experimental support. Authors would also like to

653 thank the Central Support Service for Experimental Research (SCSIE) of the University
654 of Valencia for the electronic microscopy service.

655 **REFERENCES**

656 Aceituno-Medina, M., Mendoza, S., Lagaron, J. M., & López-Rubio, A. (2013). Development and
657 characterization of food-grade electrospun fibers from amaranth protein and pullulan
658 blends. *Food Research International, 54*, 667-674. doi:
659 http://dx.doi.org/10.1016/j.foodres.2013.07.055
660 Aewsiri, T., Benjakul, S., Visessanguan, W., Wierenga, P. A., & Gruppen, H. (2010).
661 Antioxidative activity and emulsifying properties of cuttlefish skin gelatin–tannic acid
662 complex as influenced by types of interaction. *Innovative Food Science & Emerging*
663 *Technologies, 11*, 712-720. doi: http://dx.doi.org/10.1016/j.ifset.2010.04.001
664 Doyle, B. B., Bendit, E. G., & Blout, E. R. (1975). Infrared spectroscopy of collagen and collagen-
665 like polypeptides. *Biopolymers, 14*, 937-957. doi: 10.1002/bip.1975.360140505
666 Ebrahimgol, F., Tavanai, H., Alihosseini, F., & Khayamian, T. (2014). Electrosprayed recovered
667 wool keratin nanoparticles. *Polymers for Advanced Technologies, 25*, 1001-1007. doi:
668 10.1002/pat.3342
669 Gallardo, G., Guida, L., Martinez, V., López, M. C., Bernhardt, D., Blasco, R., . . . Hermida, L. G.
670 (2013). Microencapsulation of linseed oil by spray drying for functional food
671 application. *Food Research International, 52*, 473-482. doi:
672 http://dx.doi.org/10.1016/j.foodres.2013.01.020
673 Gómez-Mascaraque, L. G., Lagarón, J. M., & López-Rubio, A. (2015). Electrosprayed gelatin
674 submicroparticles as edible carriers for the encapsulation of polyphenols of interest in
675 functional foods. *Food Hydrocolloids, 49*, 42-52. doi:
676 http://dx.doi.org/10.1016/j.foodhyd.2015.03.006
677 Guillen, M., & Cabo, N. (1997). Characterization of edible oils and lard by Fourier transform
678 infrared spectroscopy. Relationships between composition and frequency of concrete
679 bands in the fingerprint region. *Journal of the American Oil Chemists' Society, 74*, 1281-
680 1286.
681 Howe, A. M., & Pitt, A. R. (2008). Rheology and stability of oil-in-water nanoemulsions
682 stabilised by anionic surfactant and gelatin 2) addition of homologous series of sugar-
683 based co-surfactants. *Advances in Colloid and Interface Science, 144*, 30-37. doi:
684 http://dx.doi.org/10.1016/j.cis.2008.08.004
685 Jaworek, A., & Sobczyk, A. T. (2008). Electrospraying route to nanotechnology: An overview.
686 *Journal of Electrostatics, 66*, 197-219. doi:
687 http://dx.doi.org/10.1016/j.elstat.2007.10.001
688 Jiménez-Martín, E., Gharsallaoui, A., Pérez-Palacios, T., Carrascal, J., & Rojas, T. (2014).
689 Suitability of Using Monolayered and Multilayered Emulsions for Microencapsulation
690 of ω-3 Fatty Acids by Spray Drying: Effect of Storage at Different Temperatures. *Food*
691 *and Bioprocess Technology*1-12. doi: 10.1007/s11947-014-1382-y
692 Kapchie, V. N., Yao, L., Hauck, C. C., Wang, T., & Murphy, P. A. (2013). Oxidative stability of
693 soybean oil in oleosomes as affected by pH and iron. *Food Chemistry, 141*, 2286-2293.
694 doi: http://dx.doi.org/10.1016/j.foodchem.2013.05.018
695 Kolanowski, W., Ziolkowski, M., Weißbrodt, J., Kunz, B., & Laufenberg, G. (2006).
696 Microencapsulation of fish oil by spray drying--impact on oxidative stability. Part 1.
697 *European Food Research and Technology, 222*, 336-342.
698 Leong, T., Wooster, T., Kentish, S., & Ashokkumar, M. (2009). Minimising oil droplet size using
699 ultrasonic emulsification. *Ultrasonics Sonochemistry, 16*, 721-727.

Long, G., Ji, Y., Pan, H., Sun, Z., Li, Y., & Qin, G. (2015). Characterization of thermal denaturation structure and morphology of soy Glycinin by FTIR and SEM. *International Journal of Food Properties, 18*, 763-774.

López-Rubio, A., & Lagaron, J. M. (2012). Whey protein capsules obtained through electrospraying for the encapsulation of bioactives. *Innovative Food Science & Emerging Technologies, 13*, 200-206. doi: http://dx.doi.org/10.1016/j.ifset.2011.10.012

Malaki Nik, A., Wright, A. J., & Corredig, M. (2010). Interfacial design of protein-stabilized emulsions for optimal delivery of nutrients. [10.1039/C0FO00099J]. *Food & Function, 1*, 141-148. doi: 10.1039/C0FO00099J

McClements, D. J. (2004). Protein-stabilized emulsions. *Current Opinion in Colloid & Interface Science, 9*, 305-313. doi: http://dx.doi.org/10.1016/j.cocis.2004.09.003

McClements, D. J. (2007). Critical review of techniques and methodologies for characterization of emulsion stability. *Critical Reviews in Food Science and Nutrition, 47*, 611-649.

McClements, D. J. (2011). Edible nanoemulsions: fabrication, properties, and functional performance. *Soft Matter, 7*, 2297-2316.

McClements, D. J. (2012). Advances in fabrication of emulsions with enhanced functionality using structural design principles. *Current Opinion in Colloid & Interface Science, 17*, 235-245.

Moomand, K., & Lim, L.-T. (2014). Oxidative stability of encapsulated fish oil in electrospun zein fibres. *Food Research International, 62*, 523-532. doi: http://dx.doi.org/10.1016/j.foodres.2014.03.054

Nagarajan, M., Benjakul, S., Prodpran, T., Songtipya, P., & Nuthong, P. (2013). Film forming ability of gelatins from splendid squid (Loligo formosana) skin bleached with hydrogen peroxide. *Food Chemistry, 138*, 1101-1108. doi: http://dx.doi.org/10.1016/j.foodchem.2012.11.069

Nagiah, N., Madhavi, L., Anitha, R., Srinivasan, N., & Sivagnanam, U. (2013). Electrospinning of poly (3-hydroxybutyric acid) and gelatin blended thin films: fabrication, characterization, and application in skin regeneration. *Polymer Bulletin, 70*, 2337-2358. doi: 10.1007/s00289-013-0956-6

Pérez-Masiá, R., Lagaron, J., & Lopez-Rubio, A. (2015). Morphology and Stability of Edible Lycopene-Containing Micro- and Nanocapsules Produced Through Electrospraying and Spray Drying. *Food and Bioprocess Technology, 8*, 459-470. doi: 10.1007/s11947-014-1422-7

Pérez-Masiá, R., Lagaron, J., & López-Rubio, A. (2014). Development and Optimization of Novel Encapsulation Structures of Interest in Functional Foods Through Electrospraying. *Food and Bioprocess Technology, 7*, 3236-3245. doi: 10.1007/s11947-014-1304-z

Rodea-González, D. A., Cruz-Olivares, J., Román-Guerrero, A., Rodríguez-Huezo, M. E., Vernon-Carter, E. J., & Pérez-Alonso, C. (2012). Spray-dried encapsulation of chia essential oil (Salvia hispanica L.) in whey protein concentrate-polysaccharide matrices. *Journal of Food Engineering, 111*, 102-109. doi: http://dx.doi.org/10.1016/j.jfoodeng.2012.01.020

Surh, J., Decker, E. A., & McClements, D. J. (2006). Influence of pH and pectin type on properties and stability of sodium-caseinate stabilized oil-in-water emulsions. *Food Hydrocolloids, 20*, 607-618. doi: http://dx.doi.org/10.1016/j.foodhyd.2005.07.004

Torres-Giner, S., Martinez-Abad, A., Ocio, M. J., & Lagaron, J. M. (2010). Stabilization of a Nutraceutical Omega-3 Fatty Acid by Encapsulation in Ultrathin Electrosprayed Zein Prolamine. *Journal of food science, 75*, N69-N79.

Wang, B., Adhikari, B., & Barrow, C. J. (2014). Optimisation of the microencapsulation of tuna oil in gelatin–sodium hexametaphosphate using complex coacervation. *Food Chemistry, 158*, 358-365. doi: http://dx.doi.org/10.1016/j.foodchem.2014.02.135

751

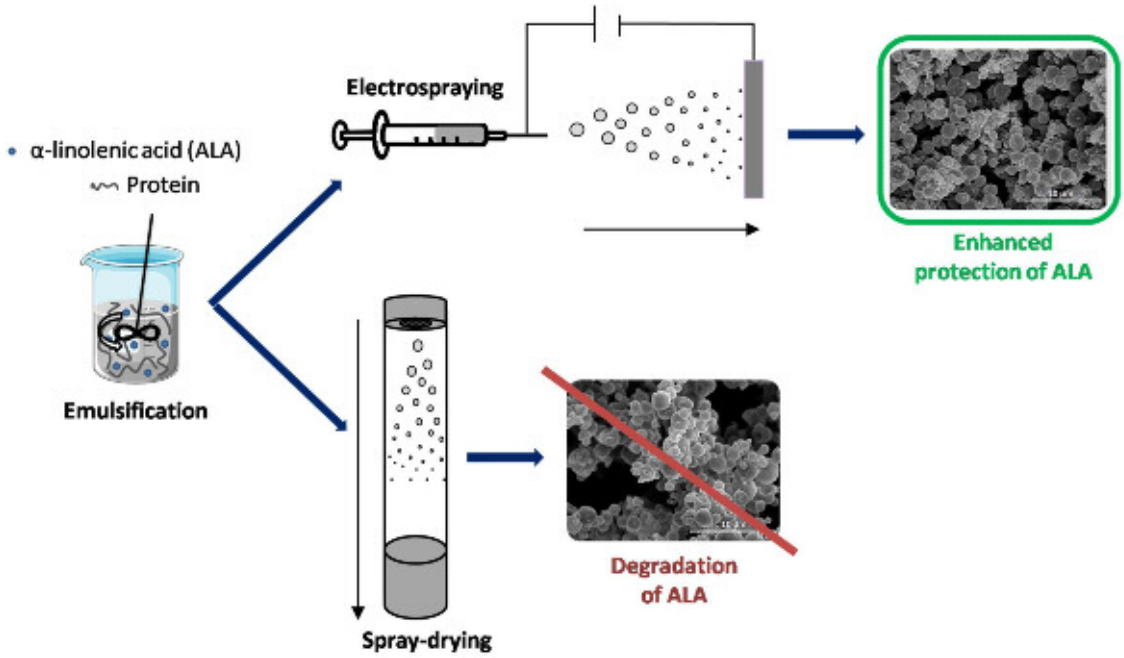

752

753 GRAPHICAL ABSTRACT